Chemical Physics 444 (2014) 43–51

Contents lists available at ScienceDirect

Chemical Physics

journal homepage: www.elsevier.com/locate/chemphys

Solid state photochromism and thermochromism of two related N-salicylidene anilines

Mihaela Avadanei [a,*], Vasile Cozan [a], Sergiu Shova [a], José António Paixão [b]

[a] "P.Poni" Institute of Macromolecular Chemistry, Iasi, Romania
[b] Faculty of Sciences and Technology, Department of Physics, University of Coimbra, Portugal

ARTICLE INFO

Article history:
Received 19 June 2014
In final form 1 October 2014
Available online 13 October 2014

Keywords:
N-salicylidene aniline
Photochromism
Thermochromism
Fluorescence
Reflectance spectroscopy

ABSTRACT

The crystalline structure and optical properties of N-salicylidene-*p*-cyanoaniline and N-salicylidene-*p*-carboxyaniline were investigated in solid state (microcrystalline powder), with the purpose to connect the effects of substitution and crystal packing with their optical properties. Diffuse reflectance and fluorescence spectroscopy were used to study the absorption and emission properties upon photoirradiation and cooling down to the liquid nitrogen temperature. The Stokes-shifted fluorescence, with a quantum yield of about 10^{-2}–10^{-1}, is given by the tautomeric *cis*-keto species formed as a result of the excited state intramolecular proton transfer from the initial enol structure. Despite their similar geometrical parameters, only SA-COOH is photochromic, which is in contradiction with literature. On the other side, the thermochromism is especially strong at SA-CN. The study shows the behavior of SA-CN similar to that of a classical anil, while SA-COOH presents interesting features that contradict the presumed behavior based only on its supramolecular structure.

1. Introduction

The ability of a molecular system to organize itself when the trigger is the light or temperature is given by a complex assembly of structural characteristics, supramolecular interactions and electronic effects on the reactive moiety. Aromatic anils, from which one can highlight N-salicylidene anilines and N-salicylidene aminopyridines, constitute a perfect example of a very versatile system with switching properties in solid state between thermo- and photochromism [1]. Due to the intramolecular hydrogen bond, these two properties are based essentially on the same phenomenon, named the tautomerism between the basic enol–imine and the keto-amine form obtained by a proton transfer from the hydroxylic group towards the imine nitrogen atom. In thermochromic crystals, the tautomeric equilibrium between the white *cis*-enol and the yellow *cis*-keto forms changes reversibly according to the temperature variation [2]. Under UV irradiation of the enol and *cis*-keto forms, the photosensitivity of crystalline anils manifests also by a change in color, but as a result of formation of the *trans*-keto isomer as ultimate and metastable photoproduct. Therefore, the photochromism consists of a succession of structural changes of the molecule, because the tautomerization must be followed by the *cis–trans* isomerization. Otherwise, the excited *cis*-keto species relaxes in a non-radiative way and no photocoloration is observed. The photochromic anils are enjoying of particular interest, because the mechanism of the intramolecular proton transfer takes place in excited state at the ultrafast time scale (from nanosecond/picoseconds in solid state [3] to femtoseconds in solution [4]), which recommends these materials in the creation of optical switches based on their nonlinear optical properties [5], data storage devices or molecular machines [6].

In crystalline state, the interplay between the two isomers is conducted by a proper manipulation of the compound structural features, by means of the so-called "crystal engineering" [7]. Thus, stabilization of a certain type of isomer can be obtained either by controlling the supramolecular architecture [8], or preparing hybrid materials by inclusion in matrices [9], co-crystallization [10] or by coordination [11]. The liaisons are the supramolecular interactions established between compound's molecules or between host and guest, with direct influence on the molecular conformation and energy levels.

Thermochromism is a general property of the salicylidene anilines (SA) derivatives, but the photochromic behavior is less encountered in solid state. Thermochromic and photochromic crystals can be then selectively designed by controlling the crystalline packing of molecules, as being stated that these two properties are mutually exclusive due to the steric requirements [1]. An

* Corresponding author.

http://dx.doi.org/10.1016/j.chemphys.2014.10.007
0301-0104/

almost planar conformation (the dihedral angle <25°) assisted by π–π or CH–π supramolecular interactions is usually consistent with a closed packed assembly and is encountered at the most of thermochromic crystals. Photochromism is associated with a twisted geometry of the molecule (the dihedral angle between the two aromatic rings >25°), therefore the molecules are less crowded and the larger space allows the isomerization towards the *trans*-keto photoproduct. This "general rule" has not been always obeyed, and interesting situations with crystals showing thermochromism and photochromism despite their closed packed structure [8d], [12], or crystals with "open – structure" but with no photosensitivity [12] were reported.

With regard to the anomalous behavior of some planar N-salicylidene anilines (SA), our study was focused on optical properties of two simple members of the SA family, which differ in substitution pattern at the aniline ring. N-salicylidene-*p*-cyanoaniline (SA-CN) and N-salicylidene-*p*-carboxyaniline (SA-COOH) are two of the simplest SAs, but the structural differences as concerning mainly the intermolecular interactions are shown to leave their mark upon photoluminescence and photochromism. Therefore, the relationship between the optical properties and the crystalline structure must be thoroughly comprehended, as most of the application ideas are focused on the use of photochromic and/or thermochromic SAs in solid state. There are several reports concerning especially the emission characteristics of SA-CN and SA-COOH. Thus, details about the excited states and the tautomerism of SA-CN in solution were obtained by time-resolved fluorometry by Vargas [13]. The emission properties of SA-COOH in crystalline state have been investigated by Chen et al., which outlined the benefits of its 1D microrod morphology as a potential optical waveguides material [14]. Johmoto et al. reported the absence of photochromism for the SA-COOH crystals, but the co-crystals of SA-COOH with some bases showed photochromic reactivity [10].

In this paper we present the results concerning the photochromism and thermochromism of SA-CN and SA-COOH obtained here by steady-state techniques and presented as a comparative analysis. The general mechanism of photo- and thermochromism, and the molecular structures are presented in Scheme 1 and in Fig. 1, respectively. Because the substitution groups at the aniline ring possess the electron – withdrawing (SA-CN) or proton donating/acceptor character (SA-COOH), the intermolecular interactions that control the supramolecular structure are different with this respect. From this reason, crystallography was used in conjunction with diffuse reflectance and emission spectroscopy in crystalline state in order to explore the thermochromic and photochromic properties of the two SAs. Although the conformation and molecular geometrical parameters are comparable, the influence of the intermolecular interactions and electronic effects is observed in their dissimilar properties mainly under photoirradiation. Our results regarding the effects of UV radiation on SA-COOH, being apparently in contradiction with those of Johmoto et. al. [10], come to add some new information concerning its photosensitivity. In the same time, no investigation on the optical properties on crystalline SA-CN has been reported, so far as we know.

2. Experimental part

2.1. Synthesis

The two compounds were synthesized in the same manner, by reacting stoichiometric amounts of salicylaldehyde or *o*-hydroxyaniline with the appropriate *p*-substituted benzaldehyde. The synthesis was performed in ethanol at room temperature for 5 h. The solvent was removed at rotavapor and the remained solid product was washed with ethanol three times, affording pure compounds as orange (SA-CN) or yellow (SA-COOH) crystalline powders. Ethanol (Chimopar SA) and the starting materials (Sigma–Aldrich) were used as received.

Characterization. Mp. (°C): **SA-CN** 123.5; **SA-COOH** > 240. ^{1}H NMR (400 MHz, $CDCl_3$, 298 K, δ ppm): **SA-CN**: 8.59 (s, 1H, CH=N), 7.71 (d, 2H, *ortho* to –CN, J 8.0 Hz), 7.44–7.40 (d, 1H, *ortho* to –CH=, J 8.0 Hz, t, 1H, *metha* to –CH=, J 8.0 Hz), 7.32 (d, 2H, *ortho* to –N=, J 8.0 Hz), 7.03 (d, 1H, *ortho* to –OH, J 8.0 Hz), 6.96 (t, 1H, *para* to –CH=, J 8.0 Hz). **SA-COOH**: 8.64 (s, 1H, CH=N), 8.16 (d, 2H, *ortho* to –COOH, J 8.0 Hz), 7.43–7.40 (d, 1H, *ortho* to –CH=, t, 1H, *metha* to –CH=), 7.33 (d, 2H, *ortho* to –N=, J 8.0 Hz), 7.04 (d, 1H,

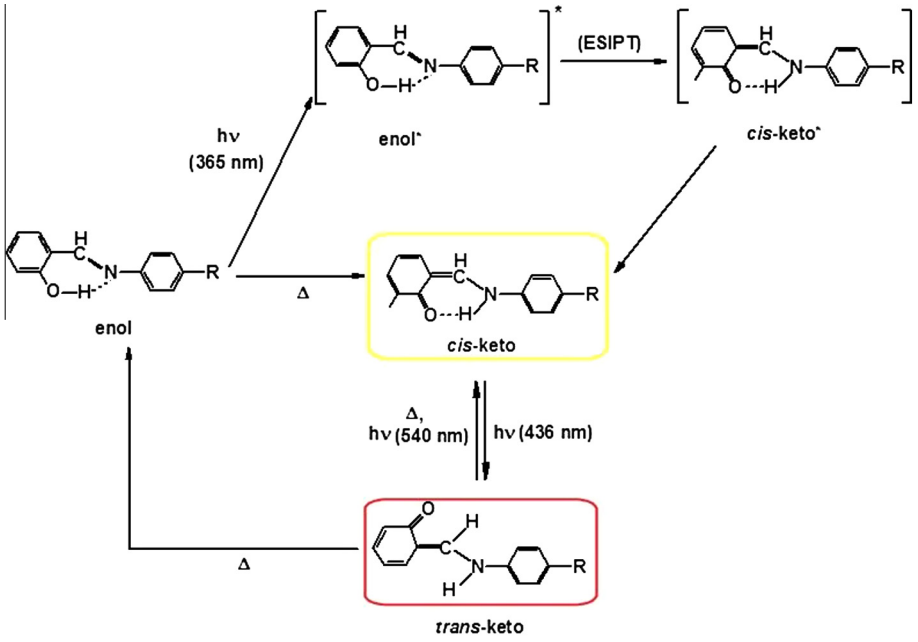

Scheme 1. The structural formulae of the two N-salicylidene derivatives studied and the activation pathways leading to thermochromism and photochromism, with the values of the irradiation wavelengths used in this study.

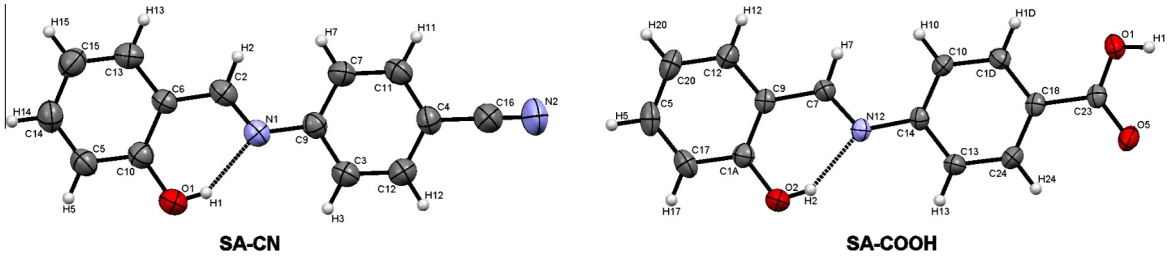

Fig. 1. ORTEP drawings at 50% probability level of the asymmetric part of the unit cell of SA-CN and SA-COOH, with the atom numbering scheme.

ortho to –OH), 6.97 (t, 1H, *para* to –CH=). FTIR (KBr, cm^{-1}): **SA-CN**: 2227 (s, C≡N), 1617 (s, C=N), 1595 (s), 1564 (s), 1489 (m), 1454 (s), 1392 (m), 1360 (m, C-Ph), 1274 (s), 1190 (m, N-Ph),1172 (s), 1151 (m), 1030 (m), 971 (m), 908 (m), 857 (s), 761 (s). SA-COOH: 3444 (br, w, OH), 1680 (s, C=O), 1621 (s, C=N), 1601 (s), 1570 (s), 1497 (s), 1458 (m), 1431 (s), 1363 (m), 1321(s), 1288 (s, C–O), 1231 (w), 1177 (s), 1160 (m), 1115 (m), 944 (m), 860 (m), 775 (s), 753 (s), 690 (m).

2.2. X-ray structure data collection and refinement

Crystallographic measurements were carried out with an Oxford-Diffraction XCALIBUR E CCD diffractometer equipped with graphite-monochromated Mo Ka radiation. Crystallinity and the crystals dimensions were checked under a polarized light microscope. The needle-like crystals suitable for single crystal X-ray diffraction studies were grown by slow evaporation from acetonitrile solution (for SA-COOH) and acetonitrile/chloroform solution (for SA-CN), at room temperature. The crystals were placed 40 mm from the CCD detector. The unit-cell determination and data integration were carried out using the CrysAlis package of Oxford Diffraction. All structures were solved by direct methods using SHELXS-9733 and refined by full-matrix least squares on Fo 2 with SHELXL-9733 with anisotropic displacement parameters for non hydrogen atoms. All H atoms attached to carbon were introduced in idealized positions using the riding model with their isotropic displacement parameters fixed at 120% of their riding atom. Positional parameters of the H attached to O atoms were obtained from difference Fourier syntheses and verified by the geometric parameters of the corresponding hydrogen bonds.

2.3. Spectral measurements

The diffuse UV–vis reflectance spectroscopy was carried out with a Specord M-200 spectrometer equipped with an integrating sphere accessory. The spectra were recorded on the pure compounds, using polytetrafluoroethylene (PTFE) as a reference. Kubelka–Munk treatment has been applied. The solid-state emission spectra were obtained with a Perkin Elmer LS55 fluorescence spectrometer and the measurements were carried out at an angle of 29° between the sample surface and the incident light beam. The fluorescence quantum yield of the powders was measured with the integrating sphere, by using an FLS908 fluorescence spectrometer (Edinburgh Instruments). The excitation source was a Xenon arc lamp at the 350 nm excitation wavelength. For both optical absorption and fluorescence measurements, the microcrystals were grinded to a fine powder.

Photoirradiation. The photochromic properties were investigated under 365 and 436 nm filtered radiation of a 350 W medium pressure mercury lamp mounted in a LOS-2 irradiation unit (Russian Federation). The radiation intensity measured at 365 nm was 7 W/m^2.

3. Results

3.1. Diffuse reflectance spectroscopy

The diffuse reflectance spectra were recorded on the powder of pure compounds, without dilution in any reference material, as being reported that the matrix effects might influence the initial equilibrium between the two tautomers [8c]. When compared to the absorption spectra of hydrocarbon and alcohol solutions, the diffuse reflectance spectra of microcrystalline powders of both compounds are extended up to 700 nm and all the electronic transitions are found to be displaced towards lower energies.

As illustrated in Fig. 2, the common feature is the region below 400 nm, where the signals from the aromatic transitions, originating from aniline and salicylidene rings, are located at the same wavelength for both compounds, i.e. 266 nm and 342 nm. Beyond 400 nm, the spectra show the differences in the electronic transitions given by the substitution and by the molecules confinement in the crystalline lattice. The broadness of the absorption bands and the peaks locations indicate the existence of intermolecular interactions and the formation of molecular aggregates in the microcrystalline powder. In addition, for both compounds one cannot exclude the possible co-existence of the enol and a trace of *cis*-keto species. The last ones, in equilibrium with the zwitterionic resonance structure, are reported as being especially stabilized in crystals [15]. The generally assigned enol region is situated in the UV domain, so the $S_1 \leftarrow S_0$ (π^*, π) transition connected to the closed form absorption is observed through the intense peak at 428 nm for SA-CN and the shoulder around 450 nm for SA-COOH. These values correspond to a spectral difference of more than 5000 cm^{-1} with respect to hydrocarbon solutions peaks. The possible contribution from the *cis*-keto species is seen in the SA-CN spectrum through the shoulder at 525 nm, fitting with the intense orange color of this compound. In turn, SA-COOH, which is bright yellow at room temperature, has the band maximum around 500 nm, also with a contribution from a trace of quinoid forms. It is worth adding that no evidence for the existence of quinoid structures in high amount was found from the SC-XRD data and from FTIR spectroscopy (Fig. S1, ESI), therefore the enol tautomer in ground state is the most stable form for the both compounds.

When subjected to photoirradiation, SA-CN and SA-COOH have been found to behave completely different, as observed by the color variations and the spectral changes associated with the chemical transformations. Irradiation of SA-CN up to 30 min, with 365 nm for 20 min and afterwards with 436 nm for 10 min more, led to no change in color and to just a weak increase of absorbance of the whole spectrum (Fig. 2(a)). The absence of photochromism at the normal time scale is then concluded for SA-CN.

In contrast, exposure of SA-COOH up to 10 min at 365 nm induced a large increase in absorbance in the whole region of the spectrum, with a special appearance of a band around 575 nm and the rising of two shoulders, around 390 and 475 nm (Fig. 2(b)). The emerging of the 575 nm and 475 nm bands

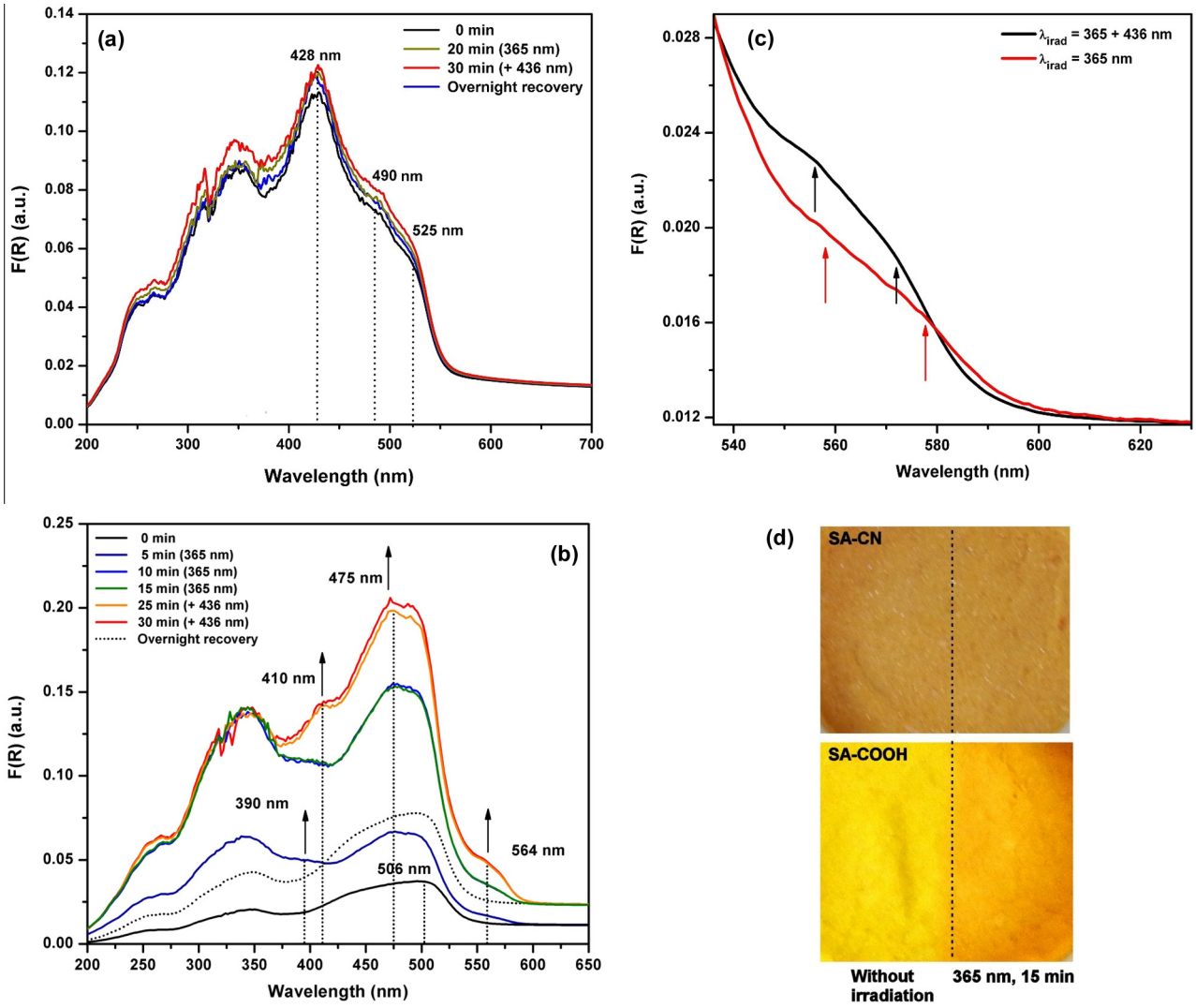

Fig. 2. Diffuse reflectance spectra during irradiation (365 nm followed by 436 nm light) at room temperature at several representative exposure times, of powders of: (a) SA-CN, and (b) SA-COOH. The arrows show the bands trend under the influence of UV radiation. The vertical dotted lines mark the peaks position. (c) The scale – expanded spectra showing the difference between the *trans*-keto form signals under the two irradiation wavelengths. (d) Photographs of SA-CN and SA-COOH powders before and after irradiation with 365 nm light.

occurred at the expenses of that at 500 nm, and, in accordance, the powder color turned from yellow to intense orange. The conversion of the closed, enolic form into the *cis*-keto form is indicated by the evolving of the 475 nm and 390 nm shoulders. The spectral changes induced by irradiation continued to show up till the exposure reached 20 min, and when the irradiation time exceeded this period the diffuse reflectance spectrum showed a photostationary state. Then, the exposure wavelength has been switched to 436 nm, in order to address the absorption of the *cis*-keto form. The spectra in Fig. 2(b) show the enhancement of the absorbance in the region assigned to the final photoproduct (564 nm) and also the formation of a weak band around 410 nm. The development of the band at 410 nm is surprising, but it is intimately correlated with that of the 564 nm envelope, as their simultaneous growth and disappearance have been observed when several cycles of irradiation/relaxation cycles have been applied. Due to the remarkable spectral changes induced in SA-COOH by irradiation, the relaxation back to the initial species was performed by monitoring the time evolution of the 564 nm band's envelope. The fading of the *trans*-keto photoproducts was seen to be almost completed in a little more than 4 h with restoring the initial yellow color.

The kinetic analysis for the fading of the 564 nm band in SA-COOH has been performed by using the Malkin equation for the first order processes, $\ln[(A_0 - A_\infty)/(A_t - A_\infty)] = k \cdot t$. Here, A_0, A_t and A_∞ are the absorbance values just when the irradiation was stopped, taken as zero time, at a time t, and in the stationary state, when the recovery of the initial state has been considered completed, respectively; k is the rate constant of the process. As it could be seen in Fig. 3, the non-linearity of the first – order plot in the two situations analyzed leads to the conclusion that the relaxation process consists of two-stage decay. The values of the rate constants are not very different each other: $k_1 = 2.31 \times 10^{-4}\ s^{-1}$ and $k_2 = 3.76 \times 10^{-4}\ s^{-1}$ for combined 365 nm + 436 nm irradiation, and $3.28 \times 10^{-4}\ s^{-1}$ and $7.04 \times 10^{-4}\ s^{-1}$, under 365 nm light only, respectively. The difference between using the two irradiation wavelengths is observed in the slower component, which decays faster under 365 nm exposure than under the combined 365 and 436 nm light. One could advance the hypothesis of two colored forms photoinduced by the two successive irradiation lights. This finding is in conjunction with the diffuse reflectance spectra (Fig. 2(c)). Here, it is observed that the additional band at 410 nm has developed only under irradiation with 436 nm and

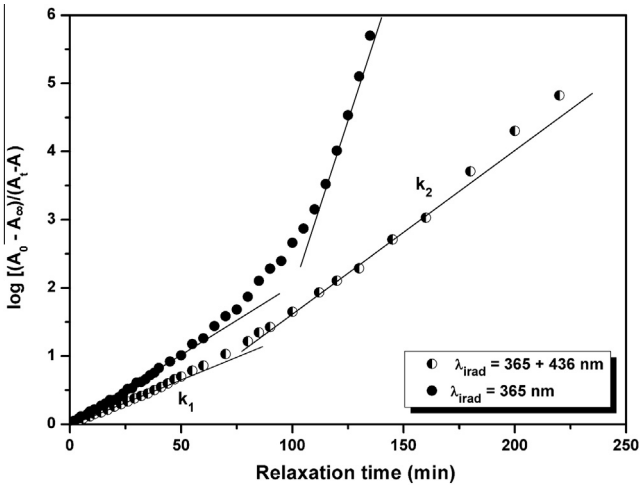

Fig. 3. Kinetic analysis by using the Malkin equation for the relaxation of the photoproduced *trans*-keto species in SA-COOH.

the centroid of the *trans*-keto band blueshifted from ≈575 nm to the final 564 nm. This suggests that the direct excitation of the *cis*-keto form would provoke the corresponding isomerization to create a second kind of *trans*-keto structures, but differing from the first ones by a small variation in conformation.

The two-stage bleaching of the photoproducts from our study is not a singular case and has been also observed for several others N-salicylidene aniline derivatives. Kawato et al. reported a similar fading process in the case of thermal relaxation of N-salicylidene aniline itself and of its deuterated derivative [16], and also for N-(3-tert-butylsalicylidene)-3-nitro-aniline [16] and 4,4′-methylenebis(N-salicylidene-2,6-diisopropylaniline) [17], or 4,4′-methylenebis{(N-3,5-di-tert-butylsalicylidene)-2,6-dimethylaniline} [18]. Since we monitored the relaxation process at 564 nm, one could ascribe the two stages of back-isomerisation to two different kinds of *trans*-keto species.

3.2. Emission properties under UV irradiation

In a close relationship with the crystalline structure, the luminescence properties of SA-CN and SA-COOH were found to be very similar prior to irradiation, but the spectral emission changes are different upon exposure to UV light. This behavior is in agreement with the photochemistry monitored by DRS (Section 3.1). The fluorescence spectroscopy in solid state has been carried out at the excitation wavelengths corresponding to the absorption of the enol and *cis*-keto tautomers, which are 350 and 500 nm, respectively.

Fig. 4 presents the emission spectra of SA-CN and SA-COOH with 350 nm and 500 nm excitation wavelength, at several representative irradiation times. The both compounds share the same profile of the fluorescence spectrum, which is slightly red-shifted for SA-CN because of the presence of the C≡N group at the para position of the aniline ring, which enlarged the conjugation and reduced the energy gap between HOMO and LUMO [19]. The emission profile consists of a single, broad and asymmetric band ranging from 500 to 700 nm, and whose intensity is higher for SA-COOH. The emission is centered at 565 nm for SA-CN and at 550 nm for SA-COOH. The quantum yields of fluorescence at the excitation wavelength of 350 nm were 0.026 for SA-CN and 0.115 for SA-COOH. The origin of the emission band is associated with the radiative relaxation of the *cis*-keto* tautomer, thus demonstrating the efficient proton transfer in the excited state.

The photoluminescence observed under photoirradiation has been monitored at 5 min time intervals. For both SA-CN and SA-COOH, the intensity of main emission peak followed an oscillatory trend, by decreasing in the first 10 min and afterwards increasing and decreasing at every 5 min of irradiation. Regardless the intensity variations as a function of irradiation time, the fluorescence spectrum of SA-CN (Fig. 4(a)) showed no visible change in shape, and the band maximum and the shoulder maintained their positions.

In contrast, the photophysics and photochemistry of SA-COOH seem to be more elaborate. As it can be observed in Fig. 4(b), under irradiation with 365 nm the decreasing of the whole emission band intensity is accompanied by the enhancement of the shoulder around 584 nm, which goes in line with the spectral changes seen in the diffuse reflectance spectra. When the sample was further subjected to the 436 nm radiation, the spectral changes consist of the reduction of the central maximum at 550 nm, the clear and continuous growing of the 584 nm emission and the appearance of a weak band in the red tail, around 630 nm.

The excitation spectra were recorded at the maximum of the emission wavelengths and are presented in Fig. 5. In the case of SA-CN (Fig. 5(a)), according to the weak modifications undergone by under 365 nm light, the excitation profiles of the 552 nm emission showed no difference before and after irradiation. Although the general profile did not entirely follow the shape of the reflectance spectrum, the positions of the peaks in the two spectra match each other. Therefore, the weak contributions at 480 and 520 nm are assigned to a trace of *cis*-keto structures, and those with much higher intensity at 417 and 370 nm come from the enol structures. It can be then safely stated that the large emission band with λ_{max} = 552 nm is arising from the radiative de-excitation of the excited *cis*-keto tautomer. The structured appearance of the SA-CN fluorescence band might be thought as originating from two different vibronic levels or could arise from radiative relaxation of two different *cis*-keto species. According to the lack of photocoloration and no evidence for a *trans*-keto* form emission, it seems that the deactivation of the *cis*-keto* state in SA-CN is not taking place by isomerisation, but through back proton transfer into the primary enol form.

As a result of the changes induced by irradiation on the relative populations of enol and keto species, the excitation spectra of SA-COOH recorded at λ_{em} = 534 nm took different shapes at different irradiation times. As one can be seen in Fig. 5(b), the contribution around 500 nm in the excitation spectrum roughly matches the corresponding peak in the reflectance spectrum. The excitation spectrum before irradiation consists of three bands, where those attributable to the *cis*-keto form (≈470 nm) and the closed enol form (420 nm) are slightly blueshifted as compared to the bands obtained in reflectance. Under irradiation with 365 nm light one can be noted the broad band in the visible region probed, which presents several unresolved contributions. The weaker band centered on 500 nm can be assigned to the *cis* open form, by comparing it to the reflectance spectrum. The wide band below 420 nm covers the region assigned to the enol form absorption.

3.3. Fluorescence studies in solid state at 77 K

The almost planar conformation of SA-CN and SA-COOH molecules could be regarded as a prerequisite for thermochromism, as a general rule in the case of SA derivatives. Therefore, the tautomeric equilibrium between the closed and open structures was investigated on cooling from room temperature down to liquid nitrogen temperature. The intense orange color of the microcrystalline powder of SA-CN at ambient temperature changes to light yellow at 77 K (Fig. 6(c)). The thermal relaxation is quite fast, the restoring to the original color being completed in a few minutes. SA-COOH behaves in a similar fashion on cooling and on thermal recovery.

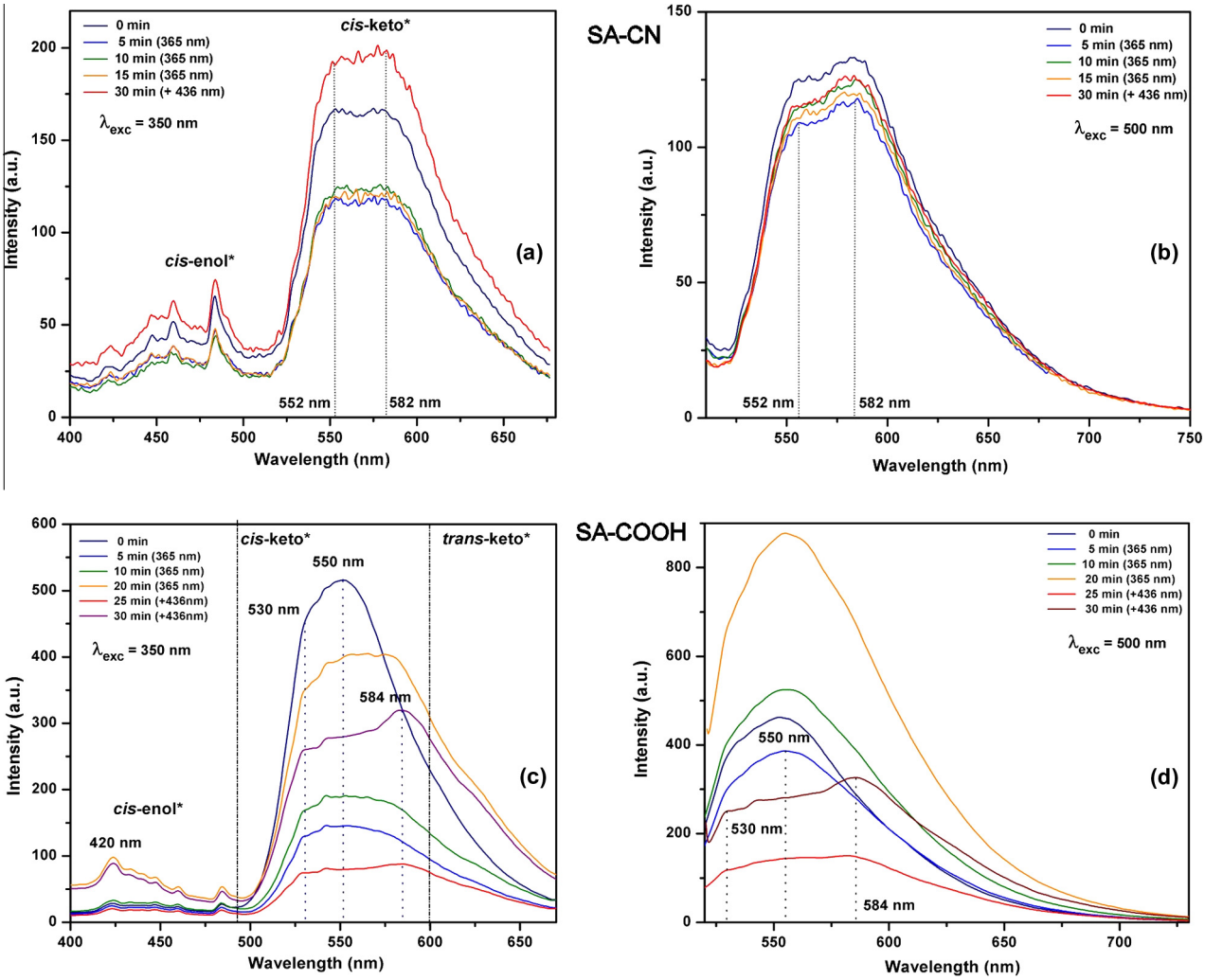

Fig. 4. Fluorescence emission spectra, excited with 350 nm (left) and 500 nm (right) under UV irradiation of microcrystalline powders of: SA-CN (a, b) and SA-COOH (c, d). The samples were irradiated with 365 nm and afterwards with 436 nm light.

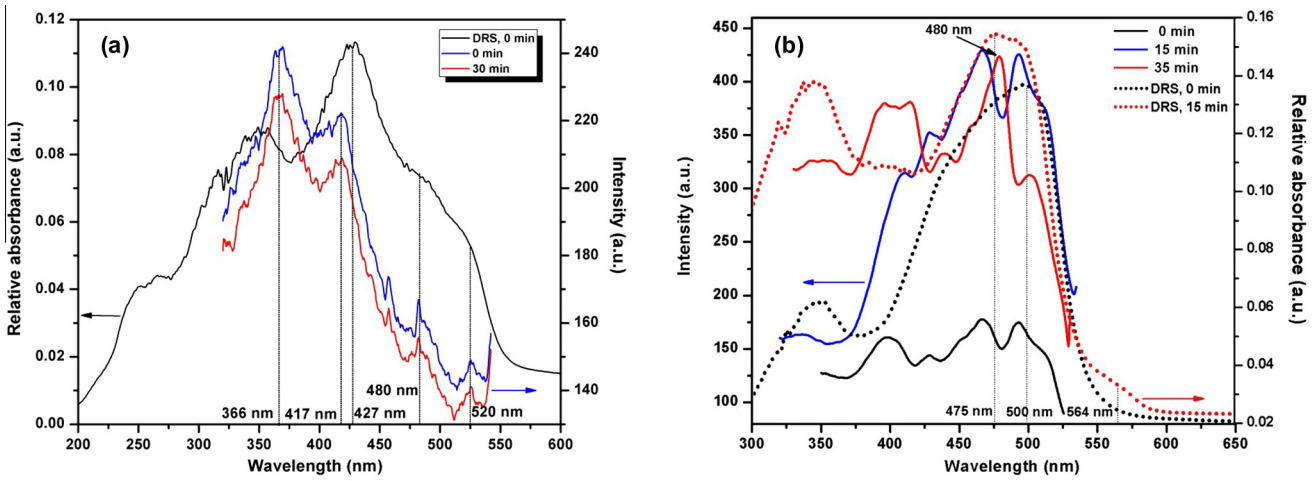

Fig. 5. (a) The excitation spectra of SA-CN at room temperature, recorded at the emission wavelength of 552 nm before (blue trace) and after irradiation (red trace), as compared with the corresponding diffuse reflectance spectrum (black trace); (b) The profiles of excitation spectra in solid state of SA-COOH, at several irradiation times, recorded at the emission wavelength of 534 nm at room temperature. The traces at 5 and 15 min were obtained under 365 nm irradiation, while that at 30 min is recorded with 20 min under 365 nm and then under 436 nm light for 10 min longer (see details in text). In comparison with the excitation spectra, the diffuse reflectance spectra before irradiation and after 15 min under 365 nm are presented with dotted lines. (For interpretation of the references to color in this figure legend, the reader is referred to the web version of this article.)

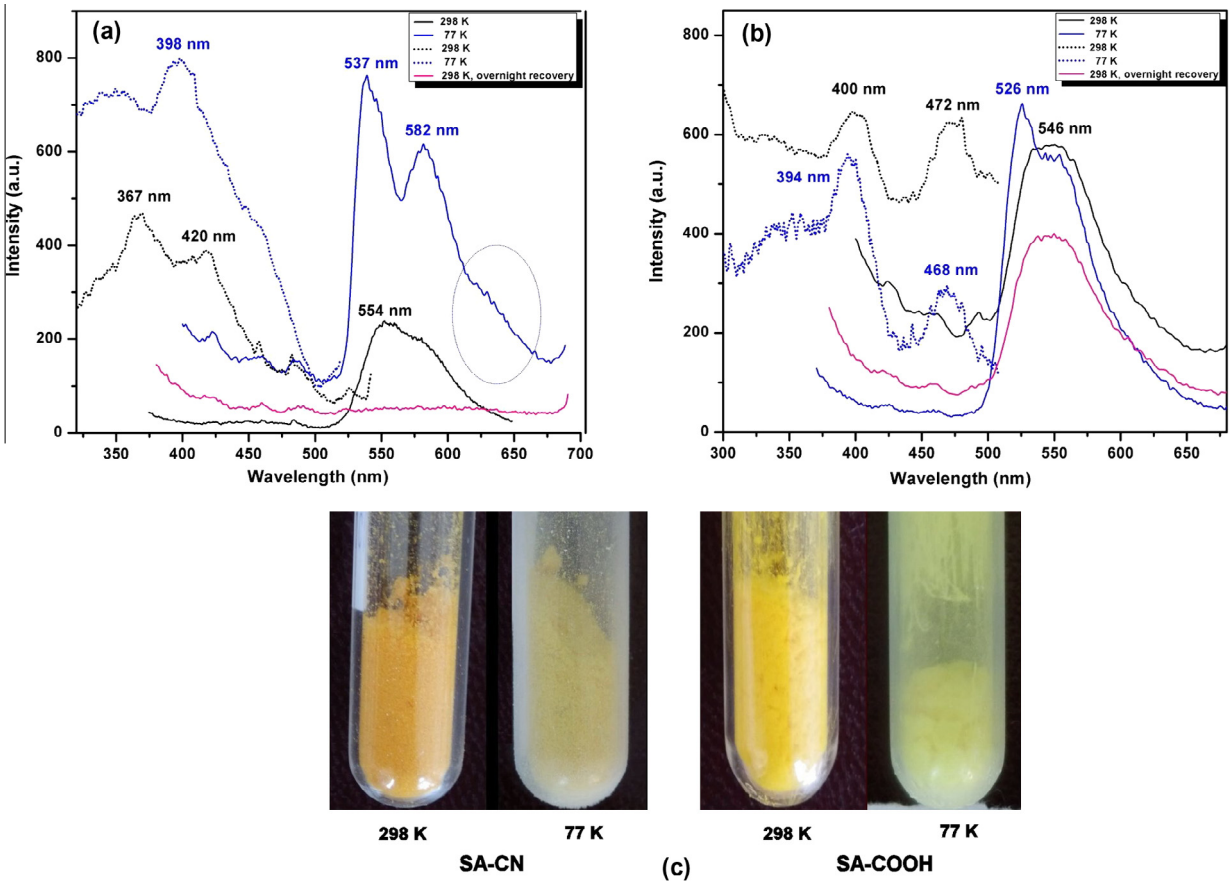

Fig. 6. The solid state emission spectra of (a) SA-CN and (b) SA-COOH, as follows: at 298 K (black trace), 77 K (blue trace) and back recovery (red trace), together with the corresponding excitation spectra (with dotted lines), observed at 554 nm (a) and 546 nm (b), respectively. (c) Photographs of powders of SA-CN and SA-COOH at two different temperatures. (For interpretation of the references to color in this figure legend, the reader is referred to the web version of this article.)

The thermo-induced structural changes were expected to be seen also in emission properties. The excitation wavelength was 350 nm, which corresponds to the maximum of the enol absorption.

In the low temperature spectrum of SA-CN (Fig. 6(a)), the band profile is similar to those reported for other SAs [20]. The fluorescence intensity increased of about 3 times and the vibronic structure of the emission band is now resolved, together with a blue shift of the high energy maximum and with the edge sharpening in the same region. This contribution is due to the radiative de-excitation of the *cis*-keto* species. The energy difference between the two resolved peaks (537 and 587 nm) is about $1440 \pm 100\ cm^{-1}$, which corresponds to an aromatic stretching vibration. The whole profile change of emission is accompanied by the enhancement of a shoulder around 628 nm, which is the thermochromic band and is indicated by a dotted ellipse in Fig 6(a).

At room temperature, the SA-CN excitation spectrum of the emission maximum at 554 nm shows a broad region with two main peaks, which is extended from UV to ≈450 nm and it was already assigned to the enolic form absorption. At 77 K, the two enol peaks show a combined red shift and intensity changes, which seems to be connected with the splitting of the main emission band. The *cis*-keto trace in ground state decreased on cooling and the increased intensity of the enol excitation band at low temperature is in accordance with the color whitening, therefore the shifted tautomeric equilibrium towards the enol species at 77 K is clearly evidenced. High temperatures are favorable to the transfer of the hydrogen atom along the O1–H1···N1 bond, giving rise to a small amount of the *cis*-keto tautomer. All these changes are accompanied by an enhancement of the Stokes shift when the temperature increased.

In the emission spectrum of SA-COOH, the two peaks are less resolved. The peak on the low energy wing is best seen by Gaussian spectral decomposition and is almost in the same position with the maximum of the band at 293 K, i.e. at 546 nm. The calculated spectral distance between the two peaks is 980 cm^{-1}. In the excitation spectra at the two different temperatures, the band around 470 nm that could be assigned to a small population of *cis*-keto species in ground state decreased on cooling. Accordingly, the enol excitation band at 400 nm increased when the temperature was lowered, so that the tautomeric equilibrium shifts towards enolic form at 77 K.

4. Discussion

The two N-salicylidene aniline derivatives analyzed show different optical properties, which may seem surprising if only their similar structural characteristics are taken into account. Apparently, SA-CN is behaving like a classical anil, showing only thermochromism and no observable photochromism in powder form. Microcrystalline SA-COOH presents both thermo- and photochromism, although it was claimed the absence of its photosensitivity [10]. Moreover, its fluorescence at room temperature is stronger as compared to that of SA-CN, while in cold conditions, the situation is reversed.

The internal H-bond is a prerequisite for the proton transfer and the further tautomerization from the initial enol-imine into the keto-amine form upon photoexcitation. The emission peaks

observed above 500 nm for both SA-CN and SA-COOH are consistent with the radiative relaxation of an excited *cis*-keto species created through the excited state intramolecular proton transfer, therefore the ESIPT process is extremely effective in both compounds. In a smaller amount, some *cis*-keto* structures produced from the direct excitation of the *cis*-keto species in ground state also show a radiative deactivation.

The color change for both compounds when the temperature was lowered is connected with the splitting of the emission band. The two resolved maxima of SA-CN fluorescence band may originate from two different conformations as regarding the molecule planarity [20]: the more planar, but less relaxed conformation fluoresces at the higher energy side, i.e. emits a pure emerald green color at 537 nm, and becomes visible when the temperature is lowered. The other *cis*-keto form is characterized by a more stable and relaxed conformation and this structure could be observed by the corresponding emission maximum at 582 nm, which maintained its position from the room temperature. The transfer of the hydrogen atom is thermally activated for both SA-CN and SA-COOH so we can conclude their similar thermochromic behavior. The thermochromic emission band that emerges around 628 nm only for SA-CN at 77 K might be given by a *cis*-keto* species with the lowest energy, therefore it must have the most stable conformation. The origin of the 628 nm band is yet to be clarified.

The lack of sensitivity of SA-CN to the irradiation with 365 nm could lead to the conclusion that the photo- and thermochromism are mutually exclusive properties in its case and the *cis–trans* isomerisation is prohibited. We cannot disregard the possibility that the photochromic cycle in the case of SA-CN is actually occurring at an ultrafast time scale. In contrast, the photochromism of SA-COOH apparently follows the general rule of the photoreactivity of N-salicylidene anilines, despite of the SA-COOH planar geometry and the tight supramolecular arrangement. In addition, the strong fluorescence and the photochromism of SA-COOH could be viewed as antagonistic properties, as the isomerization into the *trans* form is an alternative route in the *cis*-keto* relaxation and it means the quenching of fluorescence.

Therefore, the reason behind the different photochromic properties must be looked for in the supramolecular architecture and environment of the molecules. According to single crystal X-ray diffraction data, the geometrical parameters are similar for the two compounds. The dihedral angle between the two aromatic rings is of close values (6.2(4)° for SA-CN and 7.8(3)° for SA-COOH), while the crystalline packing shares as well comparable values of the interplanes distances between two stacked molecules in the cell unit (3.42 Å in SA-CN and 3.48 Å in SA-COOH). The stronger intramolecular hydrogen bond of SA-COOH (1.86 Å) as compared to that of SA-CN (1.88 Å) and the smaller values of the bonds lengths that compose the pseudo-cycle show a strained configuration. The intramolecular pseudo-cycle in the SA-CN molecule is a little more relaxed. So, the close packing leaving no virtual room for the *cis–trans* isomerization combined with the molecules planar conformation was initially seen as a strong indication of the probable absence of photochromism in solid state for both SA-CN and SA-COOH.

Therefore, one step closer into revealing the opposed photobehavior of SA-CN and SA-COOH may stem in analyzing the nature of intermolecular interactions in crystalline structure. SA-CN packing is driven by two strong π–π stacking interactions, while two individual molecules are coupled by dipolar interactions. This closed – packed arrangement of SA-CN molecules in the crystal hinders the C2–N1 torsional motion or the rotations around the C2–C6 and/or N1–C9 bonds in the *cis*-ketone form that would render the final photochromic product. Therefore, at the first glance, the π–π interactions abolished the photochromism. Moreover, the extended π conjugation across the entire molecule, given by the presence of the terminal cyano group, would allow SA-CN acquiring of a higher structural rigidity by suppressing the rotation around the C2–C6 bond, also showed by the lower value of the dihedral angle between the salicylidene and aniline rings, as compared to that in SA-COOH. This fact implies that the increased rigidity would results in a higher fluorescence yield, because the non-radiative decay of the *cis*-keto* state would have been reduced. The positive thermobehavior of SA-CN points to the existence of a small population of *cis*-keto structures in ground state at room temperature, and the thermo-induced discoloration results in converting them into the initial enol–imine structure at nitrogen liquid temperature. However, the number of molecules in the *cis*-ketone configuration is very small, as supplementary confirmed by the SC-XRD data.

In contrast, the SA-COOH molecules are stacked by means of one CH–π contact assisted by two strong O–H···H bonds between two in line/adjacent molecules. From this point of view, one could categorize the SA-COOH structure to a more "open" and relaxed kind, even when the interplanes distance is smaller than that of SA-CN and is corresponding to a "close-packed" configuration. Also, its density (1.411 g/cm^3) is greater than that of SA-CN (1.252 g/cm^3), and that would normally correspond to a crowded molecular arrangement. Because of the COOH terminal group, the π-conjugation is limited only at the salicylidene ring level, and the molecule is less rigid than SA-CN's, but it seems improbable that the close contact between the molecular layers would provide the necessary space for the free rotation of the C7–N12 plane or around the C7–C9 bond. The *cis–trans* isomerisation is going along with a quite efficient emission, showed by the 2 order of magnitude difference between the values of quantum yield of SA-COOH and SA-CN. Preliminary studies by means of time resolved fluorescence spectroscopy measured using the TCSPC technique revealed the radiative rate constants of close values for SA-COOH and SA-CN (0.0474 ns^{-1} and 0.0336 ns^{-1}, respectively), while the non-radiative rate constant of SA-COOH is almost 2.5-fold lower than that of SA-CN (0.521 ns^{-1} as compared with 1.277 ns^{-1}) [22]. This finding supports the less fluorescent character of SA-CN. Therefore, SA-COOH is behaving like a very efficient thermochromic and photochromic SA derivative. One can tentatively explain the photochromism by the creation of the red photoproduct through the "pedal motion" process, as it has been stated for the most SA derivatives [21], because of the little available space in the crystal. The studies aiming to go deep into the ultrafast processes and photophysics of SA-CN and SA-COOH through time resolved spectral methods are currently undertaken in our laboratory.

The photosensitivity of SA-COOH, in contradiction with the report of Johmoto et. al. [10], improves its capability of tuning the emitting properties by "crystal engineering". However, the changes from the planar to a non-planar conformation do not guarantee a photochromic crystal. The threshold value for the dihedral angle necessary for a SA derivative to show photochromism has been stated to be around 30° [23]. This is because the optical properties, in fact the balance between the radiative and non-radiative decay routes, are depending of many factors and the large dihedral angle between the aromatic rings is not the key factor in the SAs photosensitivity. The *cis–trans* isomerization may occur even in crowded surroundings, if the molecular environment allows the twisting motions of the C–Ph and N–Ph bonds.

5. Conclusion

Two salicylidene anilines derivatives, N-salicylidene-*p*-cyanoaniline (SA-CN) and N-salicylidene-*p*-carboxyaniline (SA-COOH), have been investigated in solid state with the purpose of getting a closer picture of their photophysical properties. The planar

conformation of both compounds constitutes a necessary but not a sufficient ground for exhibiting thermochromic properties. The crystalline arrangement of SA-CN is governed by secondary interactions between the terminal cyano group, supplemented by two π–π interactions which promote a closed packing of molecules. As for SA-COOH, two strong intermolecular hydrogen bonds and one CH–π interaction are the basis for a more relaxed packing structure.

The diffuse reflectance spectroscopy showed the presence of aggregates at room temperature, for both SA-CN and SA-COOH. The compounds showed a moderate fluorescence in solid state at room temperature, which gets stronger once the temperature was lowered (77 K), accompanied by a markedly change of color, especially in the case of SA-CN. The anomalous Stokes shift of the emission band with respect to the absorption of the enol form was explained by the radiative deactivation of the excited *cis*-keto species. These structures originate from a fast intramolecular proton/hydrogen atom transfer (ESIPT) from the initial phenol-imine to a keto-amine form.

The studies revealed the dissimilar behavior of SA-CN and SA-COOH under UV irradiation and on cooling down to nitrogen liquid temperature. The both compounds display thermochromism, as expected for the salicylidene anilines in crystalline state, but only one is also photochromic. The thermal relaxation back to the room temperature was fast, with the restoration of the initial state in a few minutes, while the lifetime of the photochromic form upon irradiation was as long as several hours. The weak thermochromic character resides in equilibrium of the major population of molecules in initial enol state with a very small population of molecules in a *cis*–keto state. The photochromic behavior of SA-COOH was tentatively explained by involving the "pedal motion" of the N7–C12 bond.

Conflict of interest

The authors declare they have no conflicts of interest to disclose.

Appendix A. Supplementary data

Supplementary data associated with this article can be found, in the online version, at http://dx.doi.org/10.1016/j.chemphys.2014.10.007.

References

[1] (a) E. Hadjoudis, I.M. Mavridis, Chem. Soc. Rev. 33 (2004) 579;
(b) K. Amimoto, T. Kawato, J. Photochem. Photobiol., C 6 (2005) 207.
[2] (a) K. Ogawa, Y. Kasahara, Y. Ohtani, J. Harada, J. Am. Chem. Soc. 120 (1998) 7107;
(b) T. Fujiwara, J. Harada, K. Ogawa, J. Phys. Chem. B 108 (2004) 4035.
[3] M. Sliwa, N. Mouton, C. Ruckebusch, S. Aloïse, O. Poizat, G. Buntinx, R. Métivier, K. Nakatani, H. Masuhara, T. Asahi, J. Phys. Chem. C 113 (2009) 11959.
[4] (a) S. Mitra, N. Tamai, Phys. Chem. Chem. Phys. 5 (2003) 4647;
(b) J.M. Ortiz-Sánchez, R. Gelabert, M. Moreno, J.M. Lluch, J. Chem. Phys. 129 (2008) 214308;
(c) M. Sliwa, N. Mouton, C. Ruckebusch, L. Poisson, A. Idrissi, S. Aloïse, L. Potier, J. Dubois, O. Poizat, G. Buntinx, Photochem. Photobiol. Sci. 9 (2010) 661.
[5] (a) M. Sliwa, S. Létard, I. Malfant, M. Nierlich, P. Lacrois, T. Asahi, H. Masuhara, P. Yu, K. Nakatani, Chem. Mater. 17 (2005) 4727;
(b) A. Plaquet, M. Guillaume, B. Champagne, L. Rougier, F. Mançois, V. Rodriguez, J.-L. Pozzo, L. Ducasse, F. Castet, J. Phys. Chem. C 112 (2008) 5638;
(c) M. Sliwa, A. Spangenberg, I. Malfant, P.G. Lacrois, R. Métivier, R.B. Pansu, K. Nakatani, Chem. Mater. 20 (2008) 4062;
(d) A. Patra, R. Métivier, J. Piard, K. Nakatani, Chem. Commun. 46 (2010) 6385.
[6] S. Kawata, Y. Kawata, Chem. Rev. 100 (2000) 1777.
[7] G.R. Desiraju, Angew. Chem. Int. Ed. 46 (2007) 8342.
[8] (a) E. Hadjoudis, A. Rontoyianni, K. Ambroziak, T. Dziembowska, I.M. Mavridis, J. Photochem. Photobiol. A 162 (2004) 521;
(b) A. Makal, W. Schilf, B. Kamiénski, A. Szady-Chelmieniecka, E. Grech, K. Wózniak, Dalton Trans. 40 (2011) 421;
(c) F. Robert, P.-L. Jacquemin, B. Tinant, Y. Garcia, Cryst. Eng. Commun. 14 (2012) 4396;
(d) F. Robert, A.D. Naik, F. Hidara, B. Tinant, R. Robiette, J. Wouters, Y. Garcia, Eur. J. Org. Chem. 2010 (2010) 621;
(e) F. Robert, A.D. Naik, B. Tinant, Y. Garcia, Inorg. Chim. Acta 380 (2012) 104;
(f) P.-L. Jacquemin, K. Robeyns, M. Devillers, Y. Garcia, Chem. Commun. 50 (2014) 649.
[9] (a) I. Casades, M. Álvaro, H. García, Eur. J. Org. Chem. 67 (2002) 2074;
(b) T. Haneda, M. Kawano, T. Kojima, M. Fujita, Angew. Chem. Int. Ed. 46 (2007) 6643;
(c) E. Hadjoudis, A.B. Bourlinos, D. Petridis, J. Incl. Phenom. Macrocyclic Chem. 42 (2002) 275;
(d) P.L. Jacquemin, Y. Garcia, M. Devillers, J. Mater. Chem. C 2 (2014) 1815;
(e) M. Ziółek, I. Sobczak, J. Incl. Phenom. Macrocyclic Chem. 63 (2009) 211.
[10] (a) K. Johmoto, A. Sekine, H. Uekusa, Cryst. Growth Des. 12 (2012) 4779;
(b) K.M. Hutchins, S. Dutta, B.P. Loren, L.R. MacGillivray, Chem. Mater. 26 (2014) 3042.
[11] (a) A. Kagkelari, V. Bekiari, E. Stathatos, G.S. Papaefstathiou, C.P. Raptopoulou, T.F. Zafiropoulos, P. Lianos, J. Lumin. 129 (2009) 578;
(b) F. Robert, B. Tinant, R. Clérac, P.-L. Jacquemin, Y. Garcia, Polyhedron 29 (2010) 2739;
(c) L. Chen, J. Qiao, J. Xie, L. Duan, D. Zhang, L. Wang, Y. Qiu, Inorg. Chim. Acta 362 (2009) 2327;
(d) O. Kotova, K. Lyssenko, A. Rogachev, S. Eliseeva, I. Fedyanin, L. Lepnev, L. Pandey, A. Burlov, A. Garnovskii, A. Vitukhnovsky, M. Van der Auweraer, N. Kuzmina, J. Photochem. Photobiol. A 218 (2011) 117.
[12] F. Robert, A.D. Naik, B. Tinant, R. Robiette, Y. Garcia, Chem. Eur. J. 15 (2009) 4327.
[13] (a) V. Vargas, L. Amigo, J. Chem. Soc., Perkin Trans. 2 (2001) 1124;
(b) V. Vargas C, J. Phys. Chem. A 108 (2004) 281.
[14] X.-T. Chen, Y. Xiang, P.-S. Song, R.-R. Wei, Z.-J. Zhou, K. Li, A.-J. Tong, J. Lumin. 131 (2011) 1453.
[15] K. Ogawa, J. Harada, J. Mol. Struct. 647 (2003) 211.
[16] K. Amimoto, H. Kanatomi, A. Nagakari, H. Fukuda, H. Koyama, T. Kawato, Chem. Commun. 24 (2003) 870.
[17] M. Taneda, K. Amimoto, H. Koyama, T. Kawato, Org. Biomol. Chem. 2 (2004) 499.
[18] M. Taneda, H. Koyama, T. Kawato, Res. Chem. Intermed. 35 (2009) 643.
[19] T.-C. Fang, H.-Y. Tsai, M.-H. Luo, C.-W. Chang, K.-Y. Chen, Chin. Chem. Lett. 24 (2013) 145.
[20] J. Harada, T. Fujiwara, K. Ogawa, J. Am. Chem. Soc. 29 (2007) 16216.
[21] J. Harada, H. Uekusa, Y. Ohashi, J. Am. Chem. Soc. 121 (1999) 5809.
[22] M. Avadanei, V. Cozan, C. Serpa, J. Pina, I. Tigoianu, unpublished results.
[23] K. Johmoto, T. Ishida, A. Sekine, H. Uekusa, Y. Ohashi, Acta Cryst. B68 (2012) 297.